





Cite this: *Polym. Chem.*, 2020, **11**, 439

## Synthesis of modifiable photo-responsive polypeptides bearing allyloxyazobenzene side-chains†

Wei Xiong,<sup>‡</sup> Chong Zhang,<sup>‡</sup> Xiaolin Lyu, Hantao Zhou, Wenying Chang, Yu Bo, Erqiang Chen,\* Zhihao Shen \* and Hua Lu \*

Synthetic polypeptides are important protein mimics due to their similar primary and secondary structures. Previously, the properties of polypeptides can be regulated by either introducing *N*-carboxyanhydride (NCA) stimuli-responsive moieties directly or modifiable groups for post-polymerization functionalization. Here we combine the two approaches and report the synthesis of photo-responsive and modifiable helical poly(L-glutamate) bearing an azobenzene (Azo) and an alkene (“ene”) group in the side chain, namely P(AzoEne-Glu)s. The polypeptides, prepared by the controlled ring-opening polymerization of a novel monomer AzoEne-GluNCA, undergo rapid and high yield UV-triggered *trans*–*cis* isomerization of the Azo moiety. However, this change in the primary structure does not lead to interruption of the helical secondary structure. The rigid helical main-chain and pendent Azo mesogen together endow P(AzoEne-Glu)s with liquid crystalline properties. Moreover, the “ene” group of P(AzoEne-Glu)s can be modified with thiols *via* a UV-mediated thiol–ene reaction, or quantitatively transformed to azide *via* a novel anti-Markovnikov hydroazidation approach. The newly generated azido-containing polymer can be further converted by click-type cycloaddition reactions. This work may streamline the rapid synthesis of diverse functional and stimuli-responsive polypeptides that are potentially useful for self-assembly and liquid crystalline materials.

Received 25th July 2019,  
Accepted 25th September 2019

DOI: 10.1039/c9py01106d

rsc.li/polymers

## Introduction

Synthetic polypeptides are biodegradable and biocompatible protein mimics bearing a peptide main chain and various secondary structures including  $\alpha$ -helices and  $\beta$ -sheets.<sup>1,2</sup> Owing to recent advances in controlled ring-opening polymerization (ROP) of  $\alpha$ -amino acid *N*-carboxyanhydrides (NCAs), polypeptides are playing increasingly important roles in biomedical applications such as drug delivery, gene delivery, tissue engineering, and long-acting protein therapeutics.<sup>3–9</sup> To manipulate the properties of synthetic polypeptides, many strategies have been rigorously and successfully applied in the past two decades. One of the approaches is to introduce responsive building blocks to the side chain of NCA, which gave rise to responsive polypeptides after ROP. Along this direction, many interesting polypeptides showing responsiveness to external stimuli (*e.g.*, temperature, redox, pH, and light) have been developed.<sup>10</sup>

Taking photo-responsive polypeptides as examples, common photo labile and/or switchable groups such as azobenzene (Azo),<sup>11–13</sup> coumarin,<sup>14</sup> 2-nitrobenzyl,<sup>15</sup> spiropyran,<sup>16</sup> and cinnamyl<sup>17</sup> have been implemented in NCA monomers for polymerization. Thanks to the precise spatiotemporal and remote control of the light stimulus, these materials hold great promise for applications such as photo regulated gene/siRNA transfection,<sup>18</sup> self-assembly,<sup>16,19–21</sup> and photo patterning,<sup>22</sup> *etc.* Another strategy capitalizes on post-polymerization modification for expanded repertoires of functional polypeptides.<sup>23,24</sup> Notable examples include highly efficient “click” type reactions such as copper(i)-catalyzed azide–alkyne cycloaddition (CuAAC),<sup>25</sup> thiol–yne/ene reaction,<sup>26–29</sup> Michael addition,<sup>30</sup> methionine alkylation,<sup>31,32</sup> redox transformation,<sup>33</sup> and olefin metathesis.<sup>33</sup> Despite the tremendous progress, however, there are still pressing needs for novel functionalization methods and new structures. Moreover, polypeptides simultaneously harnessing the power of both stimuli-responsiveness and post-polymerization functionalization are still sparse. To realize this goal, one must introduce both responsive and modifiable moieties to the NCA monomers, which may raise considerable synthetic challenges in molecular design and monomer purification.

Among many stimuli-responsive building blocks, Azo is a widely used photo-sensitive moiety that undergoes a reversible *trans*–*cis* transition under UV irradiation.<sup>34–37</sup> Apart from its

Beijing National Laboratory for Molecular Sciences, Center for Soft Matter Science and Engineering, Key Laboratory of Polymer Chemistry and Physics of Ministry of Education, College of Chemistry and Molecular Engineering, Peking University, Beijing 100871, China. E-mail: chemhualu@pku.edu.cn, zshen@pku.edu.cn, eqchen@pku.edu.cn

† Electronic supplementary information (ESI) available. See DOI: 10.1039/c9py01106d

‡ These authors contributed equally to this work.

photo reactivity, Azo is also a famous liquid crystalline (LC) mesogen.<sup>38–46</sup> We have previously introduced Azo and oligo (ethylene glycol) (EG<sub>x</sub>, *x* = 2, 4, and 6) to 4-aminophenylalanine derived NCAs, whose ROP has led to photo- and thermal-dual responsive polypeptides P(EG<sub>x</sub>-Azo)s.<sup>11</sup> Because the Azo building block is only one  $-CH_2-$  group away from the backbone in these polymers, the *trans* form polymer exhibited relatively low helicity, which was later completely disrupted by the *trans*-*cis* transition of Azo. Moreover, the polymers tend to form nanosized aggregates in various solvents due to their intrinsic amphiphilicity and relative rigid core (backbone + Azo). We envision that one approach to fine-tune the physicochemical properties is by adjusting the relative distance between the rigid Azo component and the polypeptide backbone.

Here, we report the synthesis of a novel L-glutamate-derived NCA monomer bearing an Azo mesogen and a modifiable alkene group in the side chain, namely AzoEne-GluNCA (Scheme 1). The ROP of AzoEne-GluNCA affords polypeptides P(AzoEne-Glu)s with a controlled molecular weight (*M<sub>n</sub>*) and narrow dispersity (*D*). P(AzoEne-Glu) demonstrates a reversibly photo-responsive switch in the primary structure but not the helical secondary structure. Lastly, we show that P(AzoEne-Glu) can be derivatized *via* the well-established thiol-ene reaction or converted to an azido group utilizing a novel protocol that has not been applied in polymer science previously.

## Materials and methods

### Materials

4,4'-Hydroxyphenylazobenzylalcohol (Azo-OH) was synthesized following procedures described previously. Anhydrous *N,N*-dimethylformamide (DMF) and hexamethyldisilazane (HMDS) were purchased from Sigma-Aldrich (St Louis, MO, USA). All

other chemicals were purchased from commercial sources and used as received unless otherwise specified.

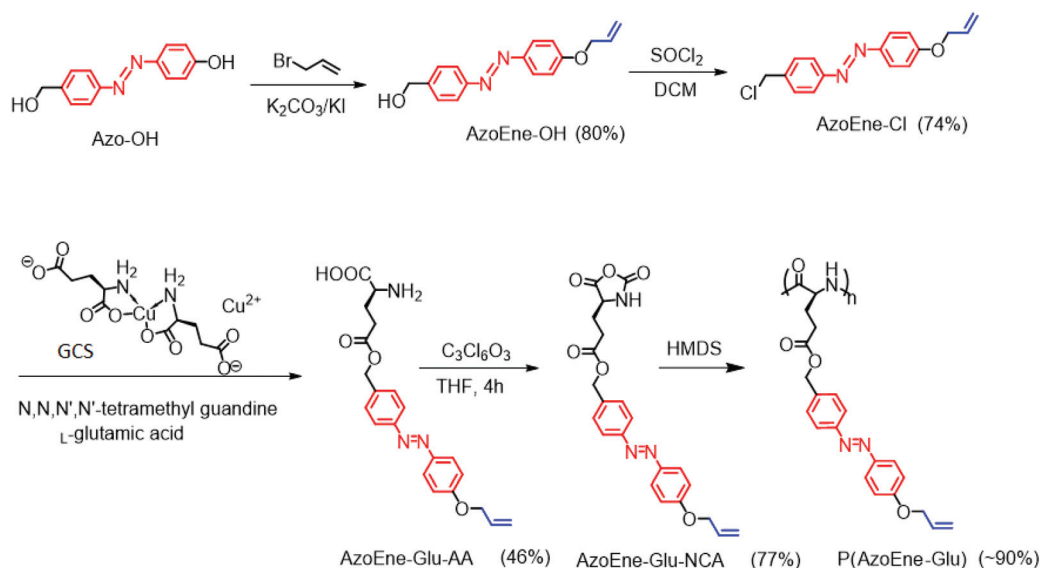
### Synthesis of 4-((4'-allyloxy) phenylazo) benzyl alcohol (Azoene-OH)

A mixture of Azo-OH (10.0 g, 43.8 mmol), allyl bromide (6.9 g, 56.9 mmol), K<sub>2</sub>CO<sub>3</sub> (7.9 g, 56.9 mmol), and KI (99.6 mg, 0.6 mmol) in anhydrous acetone (200 mL) was stirred under nitrogen for 24 h at 60 °C. The reaction mixture was filtered and the solution was evaporated to remove acetone under vacuum. The residue was dissolved in CH<sub>2</sub>Cl<sub>2</sub> (500 mL), washed with brine (100 mL), dried over Na<sub>2</sub>SO<sub>4</sub>, and concentrated under reduced pressure. The crude product was further purified by recrystallization from ethanol to give a red yellow crystal (Azoene-OH, 9.4 g, yield: 80%). <sup>1</sup>H NMR (400 MHz, CDCl<sub>3</sub>) δ 8.00–7.80 (m, 4H), 7.49 (d, *J* = 8.4 Hz, 2H), 7.10–6.96 (m, 2H), 6.08 (ddt, *J* = 17.2, 10.5, 5.3 Hz, 1H), 5.52–5.26 (m, 2H), 4.77 (s, 2H), 4.62 (ddd, *J* = 12.8, 7.1, 5.6 Hz, 2H). <sup>13</sup>C NMR (101 MHz, CDCl<sub>3</sub>) δ 161.09, 152.23, 147.07, 143.19, 132.76, 127.46, 124.74, 122.80, 118.12, 114.99, 69.06, 64.92.

### Synthesis of 4-((4'-allyloxy) phenylazo) benzyl chloride (Azo-Cl)

To an ice cooled solution of Azoene-OH (8.0 g, 29.8 mmol) in anhydrous CH<sub>2</sub>Cl<sub>2</sub> (250 mL) was added thionyl chloride (2.8 mL, 38.8 mmol) drop-wise over a period of 20 min and the mixture was stirred under nitrogen at room temperature until Azoene-OH was almost consumed as monitored by TLC (~6 h). After neutralization with saturated aqueous NaHCO<sub>3</sub>, the separated organic layer was dried over Na<sub>2</sub>SO<sub>4</sub> and evaporated off under reduced pressure. The residue was purified by column chromatography (petroleum ether/ethyl acetate, 10 : 1, v/v) to afford Azoene-Cl (6.3 g, 74%) as an orange solid.

<sup>1</sup>H NMR (400 MHz, CDCl<sub>3</sub>) δ 7.89 (dd, *J* = 19.4, 8.7 Hz, 4H), 7.51 (d, *J* = 8.3 Hz, 2H), 7.03 (d, *J* = 9.0 Hz, 2H), 6.08 (ddd,



Scheme 1 Synthesis of AzoEne-GluNCA and P(AzoEne-Glu).

$J = 22.5, 10.5, 5.3$  Hz, 1H), 5.52–5.26 (m, 2H), 4.69–4.58 (m, 4H).  $^{13}\text{C}$  NMR (101 MHz,  $\text{CDCl}_3$ )  $\delta$  161.27, 152.58, 147.05, 139.48, 132.74, 129.36, 124.88, 122.94, 118.13, 115.02, 69.07, 45.81.

### Synthesis of $\gamma$ -((4'-allyloxy) phenylazo)-L-glutamate (AzoEne-Glu)

L-Glutamic acid copper(II) complex copper(II) salt tetrahydrate (GCS) was synthesized following procedures described previously.<sup>47</sup> To a stirred solution of GCS (3.3 g, 6.7 mmol) and L-glutamic acid (2.0 g, 13.4 mmol) in mixed *N,N*-dimethylformamide (DMF)/water (12/1.9 mL), was added 1,1,3,3-tetramethylguanidine (3.4 mL, 2.7 mmol) slowly over a period of 10 min. After all solids were dissolved (~3 h), a solution of Azo-Cl in DMF (9.6 mL) was added to the deep blue solution. The mixture was further stirred at room temperature for 48 h. The slurry was added with acetone (300 mL) and kept stirring vigorously overnight until a fine precipitate was collected by centrifugation. Next, the precipitate was sonicated for 10 min in acetone and centrifuged to remove the solvent. After repeating this sonication–centrifugation procedure three times, the black green AzoEne-Glu copper(II) complex was collected and dried under vacuum. The AzoEne-Glu copper(II) complex was then added into a stirred solution of EDTA disodium salts. The black green solid gradually turned yellow and the solution turned blue. After 24 h of stirring, the solid was collected by filtration and washed with large amounts of DI water until the solid became yellow. The crude product was further recrystallized with water/isopropyl alcohol (1:2 v/v), and lyophilized to give AzoEne-Glu (3.6 g, 46% yield).  $^1\text{H}$  NMR (400 MHz, DMSO)  $\delta$  7.90 (d,  $J = 7.6$  Hz, 2H), 7.86 (d,  $J = 8.3$  Hz, 2H), 7.58 (d,  $J = 8.4$  Hz, 2H), 7.17 (d,  $J = 9.0$  Hz, 2H), 6.09 (ddd,  $J = 22.4, 10.5, 5.2$  Hz, 1H), 5.38 (ddd,  $J = 13.9, 11.8, 1.4$  Hz, 2H), 4.70 (d,  $J = 5.2$  Hz, 2H), 3.97 (t,  $J = 6.6$  Hz, 1H), 2.78–2.56 (m, 2H), 2.23–2.04 (m, 2H).  $^{13}\text{C}$  NMR (101 MHz, DMSO)  $\delta$  172.09, 170.64, 161.44, 152.04, 146.58, 139.17, 133.57, 129.26, 125.07, 122.77, 118.40, 115.76, 69.03, 65.68, 51.35, 29.71, 25.39.

### Synthesis of $\gamma$ -((4'-allyloxy) phenylazo)-L-glutamate *N*-carboxyanhydride (AzoEne-GluNCA)

AzoEne-Glu (1.0 g, 2.5 mmol) and triphosgene (276.3 mg, 0.9 mmol) were suspended in dry THF (60 mL) under nitrogen. The suspension was stirred at 50 °C for 4 h to obtain a clear solution. After the removal of the solvent under vacuum, the crude product was purified by recrystallization from THF/hexane (10/60 mL) in a glove box to yield pure AzoEne-GluNCA as a yellow powder (0.8 g, 77% yield).  $^1\text{H}$  NMR (400 MHz,  $\text{CDCl}_3$ )  $\delta$  7.91 (d, 2H), 7.88 (d,  $J = 8.3$  Hz, 2H), 7.47 (d,  $J = 8.2$  Hz, 2H), 7.03 (d,  $J = 8.9$  Hz, 2H), 6.30 (s, 1H), 6.08 (ddd,  $J = 22.5, 10.5, 5.3$  Hz, 1H), 5.39 (dd, 2H), 5.19 (s, 2H), 4.63 (d,  $J = 5.3$  Hz, 2H), 4.39 (t,  $J = 6.0$  Hz, 1H), 2.62 (t, 2H), 2.30 (ddd,  $J = 17.9, 11.7, 6.1$  Hz, 1H), 2.14 (td,  $J = 14.1, 6.9$  Hz, 1H).  $^{13}\text{C}$  NMR (101 MHz,  $\text{CDCl}_3$ )  $\delta$  172.45, 169.27, 161.29, 152.75, 151.35, 147.02, 137.17, 132.70, 129.04, 124.87, 122.87, 118.15, 115.01, 69.07, 66.69, 57.09, 30.05, 26.98. ESI-MS: calculated  $m/z$  423.4; found  $m/z$  422.3  $[\text{M} - \text{H}]^-$ .

### General procedure for the polymerization of AzoEne-GluNCA

In a glovebox, AzoEne-GluNCA (100 mg, 0.2 mmol, 50 equiv.) was dissolved in DMF (2 mL), followed by the addition of the initiator HMDS (9.6  $\mu\text{L} \times 0.5$  M, 1.0 equiv.). The polymerization solution was stirred for 30 h at room temperature. Upon completion of polymerization, acetic anhydride (9.1  $\mu\text{L}$ , 20 equiv.) was added and the solution was stirred for another 2 h before the polymer was precipitated in diethyl ether. The obtained polymer was then sonicated for 5 min in diethyl ether and centrifuged to remove the solvent. After repeating this sonication–centrifugation procedure three times, the yellow product P(AzoEne-Glu) was collected and dried under vacuum (yield ~90%).

### General procedure for the post-polymerization modification via thiol-ene reaction

P(AzoEne-Glu) (30.0 mg, 0.079 mmol “ene”), thiol molecules (7.9 mmol “thiol”), and DMPA (1.8 mg, 0.007 mmol) were dissolved in DMF (5 mL). The vial was purged with nitrogen for 10 min and sealed with a cap. The mixture was irradiated with a 365 nm UV lamp (1.0 W  $\text{cm}^{-2}$ ) overnight; to ensure complete conversion, the reaction was irradiated for another 6 h with the addition of 2 mL deionized (DI) water and 1.8 mg DMPA. The product was dialyzed against DI water and lyophilized to afford a yellow solid (typical ene conversion 70–85%).

### General procedure for the post-polymerization modification via hydroazidation reaction (Synthesis of P(AzoN<sub>3</sub>-Glu))

P(AzoEne-Glu) (15.0 mg, 0.04 mmol “ene”) and benziodoxole (27.0 mg, 0.04 mmol) were added to a 5 mL vial equipped with a stir bar. The vial was evacuated, backfilled with nitrogen, and sealed with a rubber septum. Next,  $\text{CH}_2\text{Cl}_2$  (0.2 mL) was added *via* a syringe to dissolve all substrates in the vial. Next,  $\text{H}_2\text{O}$  (18.0  $\mu\text{L}$ , 0.04 mmol) and  $\text{TMSN}_3$  (237.0  $\mu\text{L}$ , 0.4 mmol) were added to the reaction. The mixture was stirred overnight before it was dried under vacuum and redissolved in DMF. The obtained solution was dialyzed against DI water and lyophilized to afford a yellow powder product (yield ~95%).

### General procedure for post-polymerization modification via CuAAC reaction

In a glovebox, P(AzoN<sub>3</sub>-Glu) (16.9 mg, 0.04 mmol “azido”), 1-hexyne (6.6 mg, 0.08 mmol), and PMDETA (28.0  $\mu\text{L}$ , 0.20 mmol) were dissolved in DMF before CuBr (11.2 mg, 0.08 mmol) was added to the mixture. The reaction mixture was stirred at room temperature for 24 h before being quenched with 1 M HCl. The product was purified by dialysis against HAC–NaOAc buffer (pH 5) to remove copper ions in the dialysis bag with a cutoff molar mass of 1000  $\text{g mol}^{-1}$  for 3 d. The resultant solution was lyophilized to afford a yellow powder (yield ~85%).

## Results and discussion

The amino acid AzoEne-Glu containing an allyloxyazobenzene moiety was derivatized from L-glutamate in three steps as shown Scheme 1. Briefly, the compound Azo-OH containing a

phenolic hydroxyl group was reacted with allyl bromide in the presence of  $K_2CO_3$  and KI to generate **AzoEne-OH** in ~80% yield. Next, the benzyl hydroxyl of **AzoEne-OH** was chlorinated using  $SOCl_2$  to afford the compound **AzoEne-Cl** with high conversion. **AzoEne-Cl** was nucleophilically attacked by the  $\gamma$ -carboxylate of GCS to generate **AzoEne-Glu** in ~46% yield. All precursors were comprehensively characterized (Fig. S1–S6†). The obtained **AzoEne-Glu** was then cyclized using triphosgene to obtain the monomer **AzoEne-GluNCA** in anhydrous THF. The identity of **AzoEne-GluNCA** was verified by  $^1H$  and  $^{13}C$  NMR, mass spectrometry, and FT-IR as shown in Fig. 1 and Fig. S7–S8.†

Next, we conducted hexamethyldisilazane (HMDS)-mediated ROP of **AzoEne-GluNCA** to produce homo-polypeptides **P(AzoEne-Glu)**. The conversion of the monomer in DMF was monitored by FT-IR spectroscopy based on the decrease in the intensity of the anhydride  $\nu_{C=O}$  bands at 1858 and 1783  $cm^{-1}$ . The polymerization was quenched by acetic anhydride and the purified polypeptides were analyzed with size exclusion chromatography (SEC). As shown in Table 1 (entries 1–4), at a feeding monomer-to-initiator ratio (M/I) of 30/1, 50/1, 75/1 and 100/1, the obtained molecular weight ( $M_n$ ) of **P(AzoEne-Glu)** was 9.9, 20.3, 29.3 and 37.7  $kg\ mol^{-1}$ , respectively. The obtained  $M_n$ s all agreed well with the expected values. Moreover, all of the polymers showed a moderate dispersity ( $D$ ) of ~1.16–1.26 (Table 1 and Fig. S9†).

**Table 1** Size exclusion chromatography (SEC) characterization of **P(AzoEne-Glu) $_n$** <sup>a</sup>

Entry	Polymers	$M_{n-cal.}^b$	$M_{n-obt}^c$	$D^d$
1	<b>P(AzoEne-Glu)</b> <sub>30</sub>	11 400	9900	1.16
2	<b>P(AzoEne-Glu)</b> <sub>50</sub>	19 000	20 300	1.16
3	<b>P(AzoEne-Glu)</b> <sub>75</sub>	28 400	29 300	1.23
4	<b>P(AzoEne-Glu)</b> <sub>100</sub>	37 900	37 700	1.26

<sup>a</sup> Polymerizations were conducted in DMF at room temperature and characterized by SEC in DMF with 0.1 M LiBr. <sup>b</sup>  $M_{n-cal.}$  = calculated number-average molecular weight based on the feeding M/I ratio. <sup>c</sup>  $M_{n-obt}$  = obtained number-average molecular weight determined by SEC. <sup>d</sup>  $D$  = dispersity.

**P(AzoEne-Glu)s** showed excellent solubility in common organic solvents such as DMF, THF, chloroform, and dichloromethane. To study the photo-responsive behavior of **P(AzoEne-Glu)**<sub>100</sub>, we dissolved the polymer in  $CDCl_3$  and exposed the solution to 365 nm UV irradiation for 15 minutes. According to  $^1H$  NMR spectroscopy, the protons of Azo ( $H_b$  and  $H_c$ ) showed a pronounced shift from 7.68–7.74 ppm to 6.72–6.79 ppm after UV irradiation (Fig. 2B), indicating the *trans-cis* transition of Azo with a calculated conversion of ~92%. Furthermore, exposure of the UV-treated **P(AzoEne-Glu)**<sub>100</sub> to a blue LED lamp recovered the initial *trans*-form of Azo with a conversion of ~87%. The reversibility of **P(AzoEne-Glu)**<sub>100</sub> was further confirmed by UV-Vis spectroscopy. The **P(AzoEne-Glu)**<sub>100</sub> solution in THF displayed a maximal absorption peak at ~350 nm associated with the  $\pi-\pi^*$  transition of *trans*-azobenzene. The intensity of this peak gradually decreased after UV irradiation, along with a new adsorption peak emerging at ~420 nm originating from the  $n-\pi^*$  transition of *cis*-azobenzene (Fig. 2C). Interestingly, we observed a slight increase in the elution time of **P(AzoEne-Glu)**<sub>100</sub> from 29.6 to 30.0 min after UV irradiation (Fig. 3D). This minor shift suggested a decreased hydrodynamic radius derived from the *trans-cis* transformation of Azo after UV irradiation.

Next, we investigated the secondary structure of **P(AzoEne-Glu)**<sub>100</sub> in 1,1,1,3,3,3-hexafluoro-2-propanol (HFIP) solution by circular dichroism (CD) spectroscopy. As shown in Fig. 3A, the two characteristic negative peaks at 208 and 222 nm in the CD spectrum illustrated a typical  $\alpha$ -helical conformation of the polypeptide. The helicity of the polymer was calculated to be ~71% based on the intensity at 222 nm. A small couplet adsorption band was observed at ~325 and ~375 nm, likely derived from the cotton effect of  $\pi-\pi^*$  transition of Azo, suggesting a small portion of ordered alignment of the pendant azobenzene (Fig. 3A, inset). Upon UV treatment, the 325 and 375 nm peaks disappeared, which implied an order-to-disorder transition of the Azo moiety due to the *trans-to-cis* transition. To our surprise, the characteristic polypeptide helix peaks at both 208 and 222 nm did not show any sign of change, indicating that the  $\alpha$ -helix structure remained stable even though the side chain Azo switched from *trans* to *cis* conformation. This helical stability was dramatically different from our previous work on **P(EG<sub>x</sub>-Azo)s**, which showed reversible switching in both the

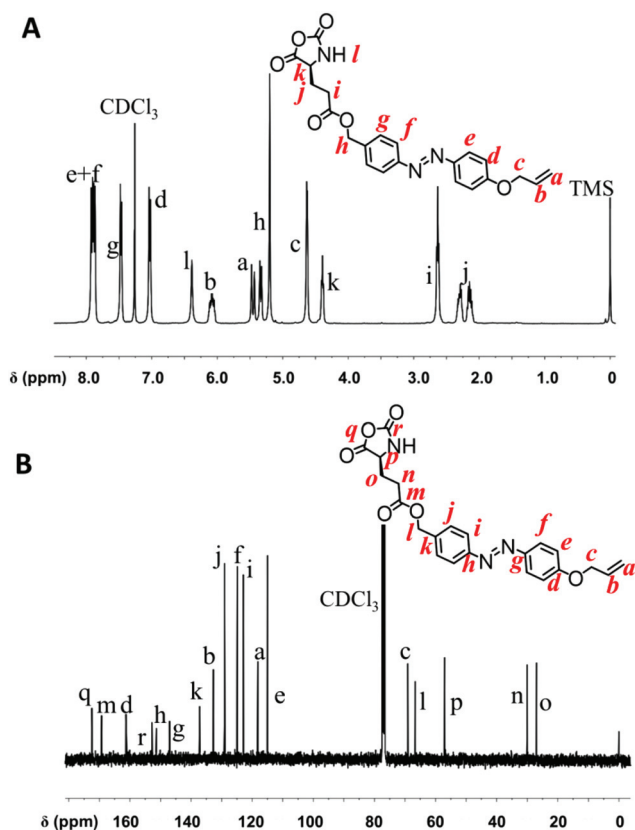


**Fig. 1**  $^1H$  (A) and  $^{13}C$  NMR (B) spectra of **AzoEne-GluNCA** in  $CDCl_3$ .

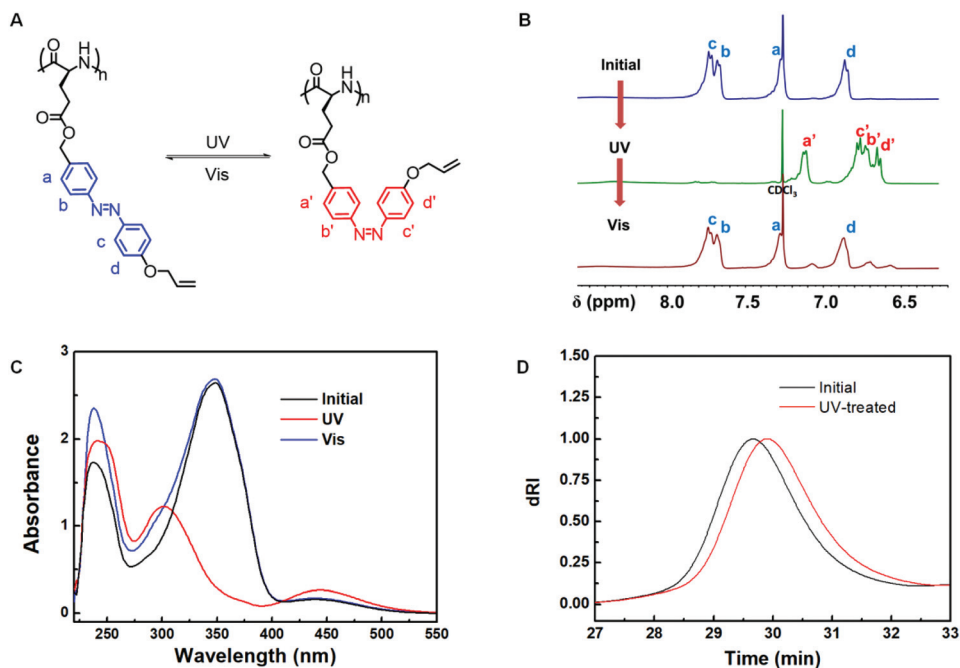


Fig. 2 Photo-responsiveness of P(AzoEne-Glu)<sub>100</sub>. (A) Scheme of the UV-triggered *trans*-*cis* isomerization of P(AzoEne-Glu)<sub>100</sub>. (B) Overlay of <sup>1</sup>H NMR spectra of P(AzoEne-Glu)<sub>100</sub> in CDCl<sub>3</sub> treated with UV (365 nm) and visible light irradiation; only the aromatic regions are shown for clarity purpose. (C) UV-vis spectra of P(AzoEne-Glu)<sub>100</sub> in THF ( $c = 0.05 \text{ mg mL}^{-1}$ ) treated with UV and visible light. (D) Overlay of SEC curves of P(AzoEne-Glu)<sub>100</sub> before and after UV irradiation.

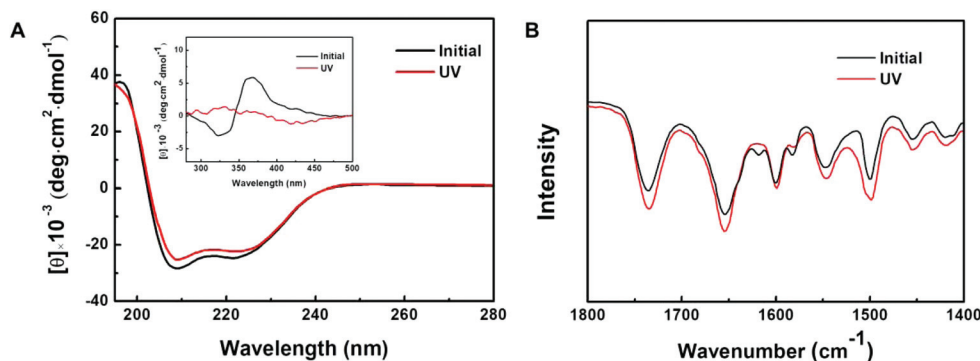
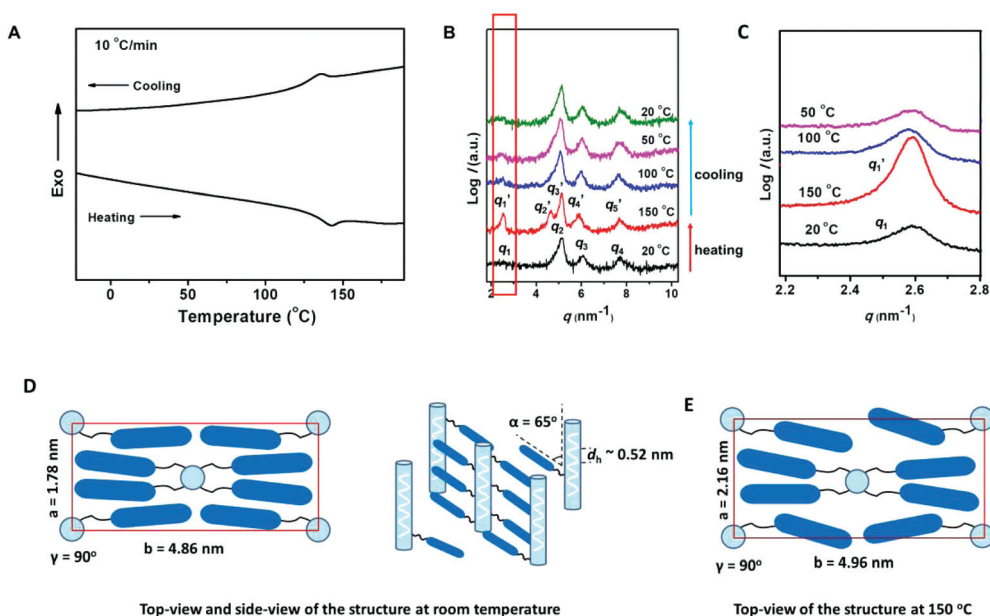


Fig. 3 Secondary structure of P(AzoEne-Glu)<sub>100</sub>. (A) CD spectra of P(AzoEne-Glu)<sub>100</sub> in HFIP. (B) FT-IR spectra of P(L-AzoEne-Glu)<sub>100</sub> in the solid state. The polymers were first irradiated with UV at 365 nm for 5 min, followed by irradiation with a blue LED for 60 min.

primary and secondary structures.<sup>11</sup> We reasoned that the relatively long linker ( $-\text{CH}_2\text{CH}_2\text{CO}_2\text{CH}_2-$ ) between the Azo and main-chain in P(AzoEne-Glu), as compared to  $-\text{CH}_2-$  in P(EG<sub>x</sub>-Azo)s, likely caused this consequence. We also tested the secondary structure of P(AzoEne-Glu)<sub>100</sub> in the solid state using FT-IR spectra. The characteristic amide I and II absorbance bands at 1546 and 1653  $\text{cm}^{-1}$  confirmed the  $\alpha$ -helix of P(AzoEne-Glu)<sub>100</sub>. No changes were observed after UV treatment, illustrating again the excellent conformational stability of P(AzoEne-Glu)<sub>100</sub> in the solid state (Fig. 3B).

To study the phase structure of P(AzoEne-Glu)<sub>50</sub>, we characterized the thermal properties of P(AzoEne-Glu)<sub>50</sub> by thermo-

gravimetric analysis (TGA) and differential scanning calorimetry (DSC) in the first step. As shown in Fig. S10,† P(AzoEne-Glu)<sub>50</sub> showed good thermal stability with the onset of weight loss (1%) temperature at  $\sim 244 \text{ }^\circ\text{C}$ . In Fig. 4A, the DSC thermograms of P(AzoEne-Glu)<sub>50</sub> showed an endothermic peak at  $\sim 140 \text{ }^\circ\text{C}$  during the heating process and an exothermic peak at almost the same temperature during the reversed cooling cycle, which together suggested a phase transition. Next, the solid state structure of P(AzoEne-Glu)<sub>50</sub> was studied by wide-angle X-ray diffraction (WAXD) and small-angle X-ray scattering (SAXS). In the low angle region of SAXS, shown in Fig. 4B-C and Table S1,† we observed four pairs of arcs on the equator at



**Fig. 4** (A) DSC curves of  $\text{P(AzoEne-Glu)}_{50}$ . (B) SAXS patterns of  $\text{P(AzoEne-Glu)}_{50}$  self-assembling at different temperatures. (C) Synchrotron SAXS patterns of  $\text{P(AzoEne-Glu)}_{50}$  self-assembling at different temperatures. (D and E) Cartoon illustration of the top-view and side-view of the ordered structure at room temperature (D) and the top-view of the structure at 150 °C (E) for  $\text{P(AzoEne-Glu)}_{50}$ .

$q_1 = 2.58 \text{ nm}^{-1}$  ( $d$  spacing of 2.43 nm),  $q_2 = 5.12 \text{ nm}^{-1}$  ( $d$  spacing of 1.22 nm),  $q_3 = 5.87 \text{ nm}^{-1}$  ( $d$  spacing of 1.06 nm), and  $q_4 = 7.67 \text{ nm}^{-1}$  ( $d$  spacing of 0.82 nm). These four peaks corresponded to (200), (400), (410), and (600) reflections of a 2D  $\text{Col}_r$  structure with  $a = 1.78 \text{ nm}$ ,  $b = 4.86 \text{ nm}$ , and  $\gamma = 90^\circ$ . The schematic illustration of this phase structure at room temperature is shown in Fig. 4D. Because the combined length of the main chain and side chain under the all-*trans* conformation was 5.13 nm, most of the flexible linkers in the side chains were expected to adopt *gauche* conformations.

Fig. 5 shows the 2D WAXD result of the sheared  $\text{P(AzoEne-Glu)}_{50}$  at room temperature with the shear direction on the meridian and X-ray beam along the  $z$ -direction. In the high-angle region, the four arcs ( $\sim 0.44 \text{ nm}$ ) marked by red ellipses

with the tilting angle at  $\pm 65^\circ$  ( $\alpha = 65^\circ$ ) in the quadrants (Fig. 5), which were easily distinguishable by angular integration, revealed that the angle between the directions of the Azo and main chain was  $65^\circ$  (Fig. 4D). These four high-angle arcs were a consequence of the interference of the layer structure composed of nematic-like Azo in each layer. Meanwhile, the two arcs ( $\sim 0.52 \text{ nm}$ ) marked by black sickles on the meridian, which were not observed in the 1D WAXD result (Fig. S11†) but became clear in the 2D WAXD after shearing, corresponded to the interference between the helices of the main chain. The  $d$  spacing value was consistent with the helical pitch of the helix (0.54 nm).

When  $\text{P(AzoEne-Glu)}_{50}$  was heated to 150 °C, five scattering peaks at  $q_{1'} = 2.53 \text{ nm}^{-1}$  ( $d$  spacing of 2.48 nm),  $q_{2'} = 4.64 \text{ nm}^{-1}$  ( $d$  spacing of 1.35 nm),  $q_{3'} = 5.12 \text{ nm}^{-1}$  ( $d$  spacing of 1.22 nm),  $q_{4'} = 5.87 \text{ nm}^{-1}$  ( $d$  spacing of 1.07 nm), and  $q_{5'} = 7.67 \text{ nm}^{-1}$  ( $d$  spacing of 0.82 nm) appeared in the low-angle region (Fig. 4B and C), which corresponded to (200), (310), (400), (410), and (600) reflections of a 2D  $\text{Col}_r$  structure with  $a = 2.16 \text{ nm}$ ,  $b = 4.96 \text{ nm}$ , and  $\gamma = 90^\circ$ . In the WAXD result, the diffraction peak at  $2\theta = 20.8^\circ$  became a halo after heating (Fig. S11†). This change indicated the disordered orientation and isotropic state of the Azo. The schematic illustration of  $\text{P(AzoEne-Glu)}_{50}$  at 150 °C is shown in Fig. 4E. It was hypothesized that the backbone of  $\text{P(AzoEne-Glu)}_{50}$  maintained a 2D  $\text{Col}_r$  structure regardless of the temperature variation, but its Azo side chain experienced an anisotropy-to-isotropy phase transition at increased temperature. The substantial increase of  $a$  and  $b$  values (Fig. 4D and E) at 150 °C could be a result of the isotropic Azo. Similar results were also observed in other main-chain/side-chain liquid crystalline polymers.<sup>48,49</sup>

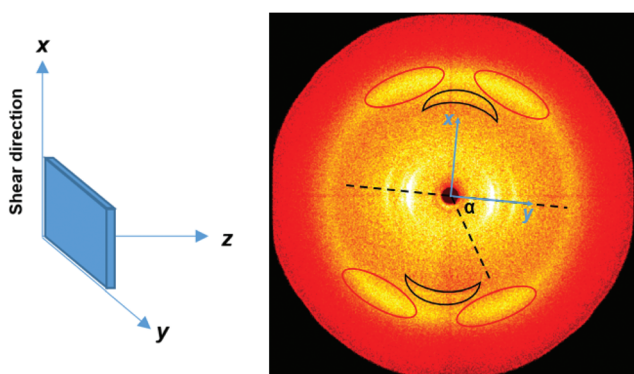


**Fig. 5** 2D-WAXD pattern of the sheared  $\text{P(AzoEne-Glu)}_{50}$  at room temperature with the shear direction on the meridian and X-ray beam along the  $z$ -direction.

To further tune the properties of **P(AzoEne-Glu)**, we explored the post-polymerization modification of the “ene” moiety. Thiol-ene of **P(AzoEne-Glu)**<sub>100</sub> with thiol molecules such as 1-hexanethiol, 2-aminoethanethiol, and sodium 2-mercaptoethanesulfonate was tested, affording polymers **P(AzoC<sub>6</sub>-Glu)**<sub>100</sub>, **P(AzoNH<sub>2</sub>-Glu)**<sub>100</sub>, and **P(AzoSO<sub>3</sub>Na-Glu)**<sub>100</sub>, respectively (Fig. 6A). Taking the reaction with 1-hexanethiol as an example, the H<sub>j</sub> peak at 5.99 ppm for **P(AzoEne-Glu)**<sub>100</sub> almost disappeared after UV irradiation (Fig. 6B, curve 2), indicating an ~88% conversion of alkene. An ~60% and >95% grafting efficiency was achieved for **P(AzoNH<sub>2</sub>-Glu)**<sub>100</sub> and **P(AzoSO<sub>3</sub>Na-Glu)**<sub>100</sub>, respectively (Fig. S12 and S13<sup>†</sup>). **P(AzoC<sub>6</sub>-Glu)**<sub>100</sub> has a good solubility in most organic solvents such as DMF, THF, chloroform, *etc.* **P(AzoNH<sub>2</sub>-Glu)**<sub>100</sub>, however, dissolved poorly in solvents such as THF, DCM, ACN, and neutral H<sub>2</sub>O. **P(AzoNH<sub>2</sub>-Glu)**<sub>100</sub> was slightly soluble in acidic solvents such as 1.0 M HCl aqueous solution and trifluoroacetic acid (TFA), likely due to the incomplete modification of “ene”. **P(AzoSO<sub>3</sub>Na-Glu)**<sub>100</sub> had a relatively improved water-solubility compared to **P(AzoNH<sub>2</sub>-Glu)**<sub>100</sub>. Similar to the unmodified neutral **P(AzoEne-Glu)**<sub>100</sub>, the anionic polypeptide **P(AzoSO<sub>3</sub>Na-Glu)**<sub>100</sub> showed an ~68% helicity, which was again found to be stable even after UV-triggered Azo isomerization (Fig. S14<sup>†</sup>). This unusual helical stability was comparable to that of those ionic helical polypeptides previously developed by Cheng *et al.*,<sup>50</sup> underscoring again the importance of the charge-backbone distance and aromatic building blocks to the helical stability of synthetic polypeptides.

The poor solubility of **P(AzoNH<sub>2</sub>-Glu)**<sub>100</sub> suggested intrinsic amphiphilicity, which stimulated us to explore its self-assem-

bly behavior. As such, we prepared an amphiphilic block copolymer **PEG5K-P(AzoNH<sub>2</sub>-Glu)**<sub>100</sub> by PEG amine ( $M_n = 5000$  g mol<sup>-1</sup>, PEG5K-NH<sub>2</sub>) initiated ROP of **AzoEne-GluNCA** and followed by thiol-ene modification with 2-aminoethanethiol (Fig. S15 and S16<sup>†</sup>). With the help of the hydrophilic PEG block, **PEG5K-P(AzoNH<sub>2</sub>-Glu)**<sub>100</sub> dispersed into water and assembled into micelles with an average particle size of ~120 nm, measured by dynamic light scattering (DLS, Fig. 6C; inset). The micellar structure was further confirmed by atomic force microscopy (AFM), and the particle sizes of micelles measured by AFM and DLS agreed well as shown in Fig. 6C. When a less polar solvent such as THF was used, we observed that **PEG5K-P(AzoNH<sub>2</sub>-Glu)**<sub>100</sub> formed 1D nanowires with an average length of ~3 μm (Fig. 6D and S17<sup>†</sup>). Moreover, when the polarity of the solvent was further decreased, **PEG5K-P(AzoNH<sub>2</sub>-Glu)**<sub>100</sub> rapidly generated an opaque organogel in DCM with a critical gelation concentration (CGC) of ~3% (Fig. 6E; inset). The AFM image illustrated the formation of a densely entangled 3D fibrous network (Fig. 6E). Although the exact mechanism is currently unclear, these results revealed that the microstructural dimension of the self-assembled **PEG5K-P(AzoNH<sub>2</sub>-Glu)**<sub>100</sub> could be regulated by the polarity of solvents.

Compared to alkyne/alkene-bearing polypeptides, azide-containing polypeptides are still rare. To our knowledge, only three examples of azide-containing NCAs were reported to date.<sup>25,51,52</sup> It would be useful to switch between functionalities so that mutually orthogonal click-like reactions can be implemented later. According to a recent study by Xu *et al.*, the anti-Markovnikov hydroazidation of alkenes with TMSN<sub>3</sub>

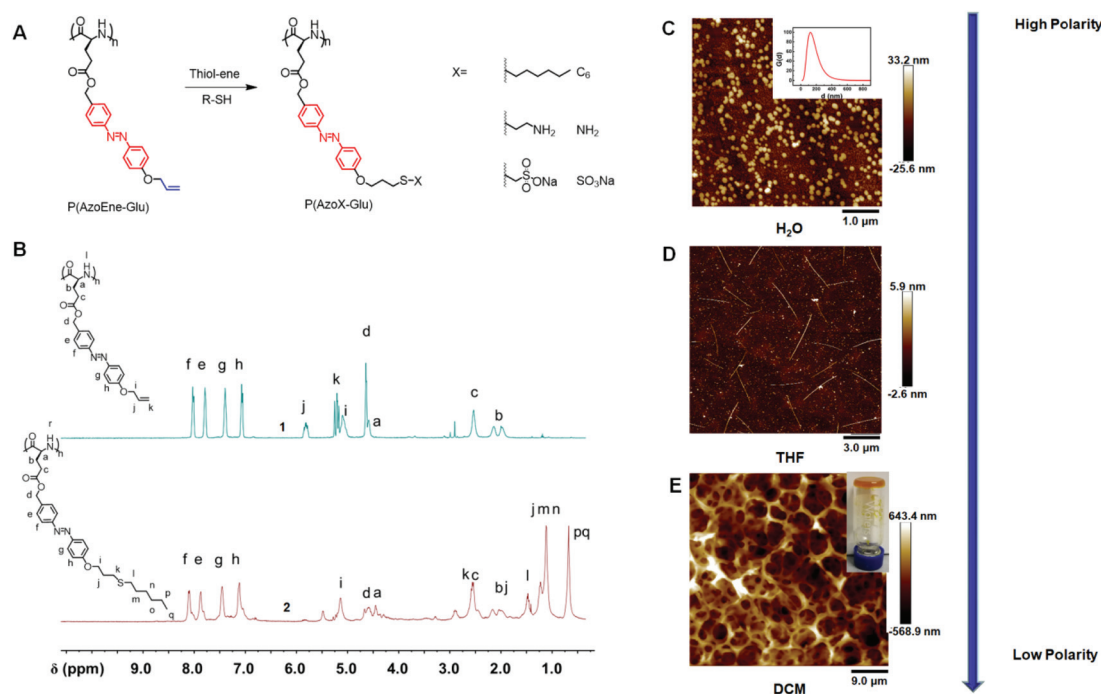


**Fig. 6** (A) Scheme of the thiol-ene reaction of **P(AzoEne-Glu)**<sub>100</sub> with various small molecule thiols. (B) Overlay of <sup>1</sup>H NMR spectra of **P(AzoEne-Glu)**<sub>100</sub> before (top) and after (bottom) the thiol-ene reaction in TFA-*d*. (C-E) AFM images of the diblock co-polymer **PEG5K-P(AzoNH<sub>2</sub>-Glu)**<sub>100</sub> self-assembled in H<sub>2</sub>O (C), THF (D), and DCM (E).

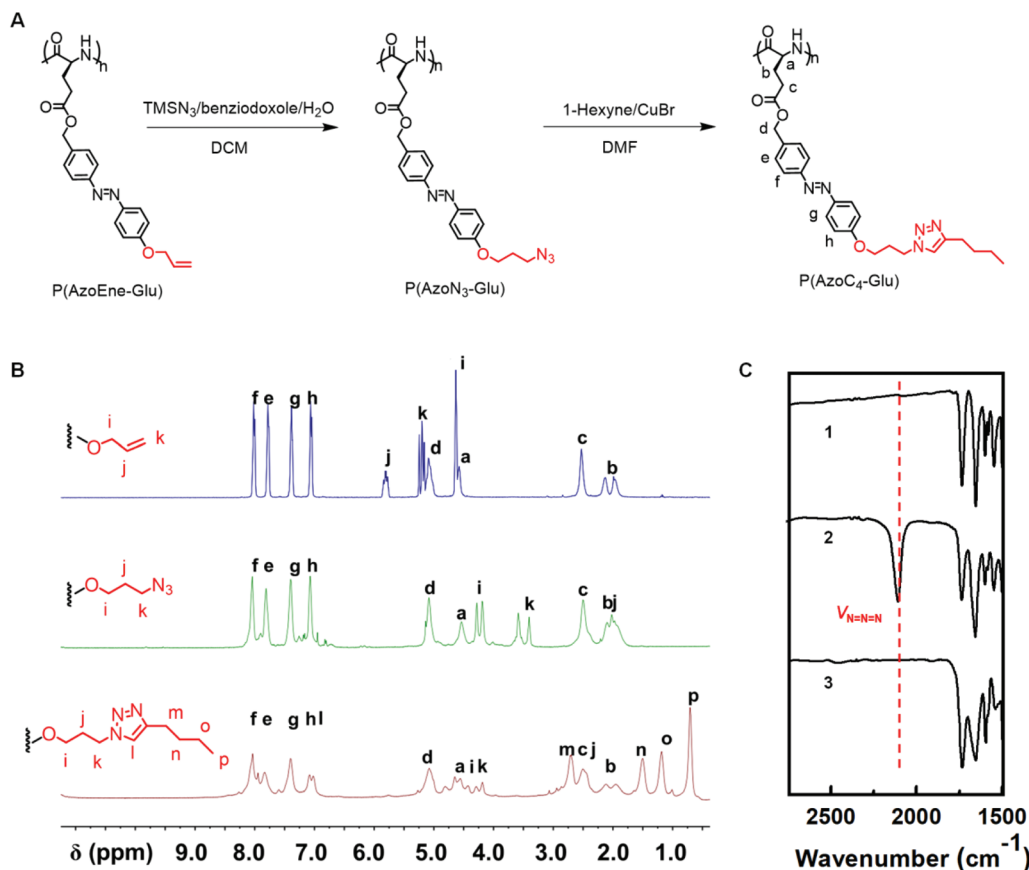


Fig. 7 (A) Scheme of the hydroazidation and subsequent CuAAC reaction of  $P(\text{AzoEne-Glu})_{100}$ . (B)  $^1\text{H}$  NMR spectra of  $P(\text{AzoEne-Glu})_{100}$  in TFA- $d$  before (top) and after hydroazidation (middle) and CuAAC reaction (bottom). (C) FTIR spectra of  $P(\text{AzoEne-Glu})_{100}$  before (spectrum 1) and after hydroazidation (spectrum 2) and CuAAC reaction (spectrum 3).

was realized using benziodoxole. However, its efficiency in the context of polymer has not been demonstrated.<sup>53</sup> Inspired by this work, we reacted  $P(\text{AzoEne-Glu})_{100}$  with  $\text{TMSN}_3$  with the catalysis of benziodoxole and water (Fig. 7A). As shown in Fig. 7B, the peaks of alkene ( $\text{H}_j$ ) at  $\sim 1.80$  ppm disappeared completely after the reaction, illustrated the full conversion of “ene” (middle). The obtained azide-containing polypeptide ( $P(\text{AzoN}_3\text{-Glu})_{100}$ ) was also verified by the characteristic absorption band at  $2090\text{ cm}^{-1}$  ( $\nu_{\text{N}=\text{N}=\text{N}}$ ) in FT-IR (spectrum 2 in Fig. 7C). Moreover, the obtained  $P(\text{AzoN}_3\text{-Glu})_{100}$  was further modifiable with an alkyne molecule *via* a CuAAC reaction. Specifically, we reacted  $P(\text{AzoN}_3\text{-Glu})_{100}$  with 1-hexyne in the presence of CuBr. The methylene protons adjacent to the azide moiety ( $\text{H}_k$ ) showed a significant shift from  $\sim 3.5$  to  $\sim 4.5$  ppm, demonstrating an almost quantitative transformation (bottom, Fig. 7B). This high efficiency was again confirmed by the disappearance of the characteristic azido band in FT-IR (spectrum 3, Fig. 7C).

affording a photo-responsive and modifiable polypeptide  $P(\text{AzoEne-Glu})$ .  $^1\text{H}$  NMR, UV-vis, and CD spectroscopy showed that the primary structure of the polypeptide experienced a *trans-cis* conversion; however, the helical structure remained unexpectedly stable after UV treatment. The pendent Azo acted as a LC mesogen in the polypeptide. The LC phase of  $P(\text{AzoEne-Glu})_{50}$  formed with the help of the interplay between the rigid helical main chain and pendent Azo. The pendent “ene” was modifiable with various thiol molecules *via* a thiol-ene reaction, and the resultant (co)polypeptides showed interesting assembly behaviours in a solvent-dependent manner. Moreover, the alkene moiety in the side chain was transformed to azide for a subsequent CuAAC reaction. Together, the monomer reported here could be a useful precursor and platform introducing various new structures. This work may streamline the rapid synthesis of diverse functional polypeptides that are potentially useful for self-assembly and liquid crystalline materials.

## Conclusions

In conclusion, we designed and synthesized a novel monomer AzoEne-GluNCA bearing an allyloxyazobenzene moiety,

## Conflicts of interest

There are no conflicts to declare.



## Acknowledgements

This work was supported by the National Natural Science Foundation of China (21434008 and 21722401).

## Notes and references

- C. Bonduelle, *Polym. Chem.*, 2018, **9**, 1517–1529.
- Z. Song, H. Fu, R. Wang, L. A. Pacheco, X. Wang, Y. Lin and J. Cheng, *Chem. Soc. Rev.*, 2018, **47**, 7401–7425.
- Z. Song, Z. Han, S. Lv, C. Chen, L. Chen, L. Yin and J. Cheng, *Chem. Soc. Rev.*, 2017, **46**, 6570–6599.
- M. A. Anderson, J. E. Burda, Y. Ren, Y. Ao, T. M. O'Shea, R. Kawaguchi, G. Coppola, B. S. Khakh, T. J. Deming and M. V. Sofroniew, *Nature*, 2016, **532**, 195–200.
- Y. Hou, J. Yuan, Y. Zhou, J. Yu and H. Lu, *J. Am. Chem. Soc.*, 2016, **138**, 10995–11000.
- Y. Hou, Y. Zhou, H. Wang, R. Wang, J. Yuan, Y. Hu, K. Sheng, J. Feng, S. Yang and H. Lu, *J. Am. Chem. Soc.*, 2018, **140**, 1170–1178.
- Y. Hou, Y. Zhou, H. Wang, J. Sun, R. Wang, K. Sheng, J. Yuan, Y. Hu, Y. Chao, Z. Liu and H. Lu, *ACS Cent. Sci.*, 2019, **5**, 229–236.
- Y. Hou and H. Lu, *Bioconjugate Chem.*, 2019, **30**, 1604–1616.
- C. Zhang and H. Lu, *Acta Polym. Sin.*, 2018, **49**, 21–31.
- J. Huang and A. Heise, *Chem. Soc. Rev.*, 2013, **42**, 7373–7390.
- W. Xiong, X. Fu, Y. Wan, Y. Sun, Z. Li and H. Lu, *Polym. Chem.*, 2016, **7**, 6375–6382.
- M. Goodman and M. L. Falxa, *J. Am. Chem. Soc.*, 1967, **89**, 3863–3867.
- M. Sisido, Y. Ishikawa, K. Itoh and S. Tazuke, *Macromolecules*, 1991, **24**, 3993–3998.
- S. Kumar, J.-F. Allard, D. Morris, Y. L. Dory, M. Lepage and Y. Zhao, *J. Mater. Chem.*, 2012, **22**, 7252–7257.
- G. Liu, L. Zhou, Y. Guan, Y. Su and C. M. Dong, *Macromol. Rapid Commun.*, 2014, **35**, 1673–1678.
- V. K. Kotharangannagari, A. Sánchez-Ferrer, J. Ruokolainen and R. Mezzenga, *Macromolecules*, 2011, **44**, 4569–4573.
- J. Ding, X. Zhuang, C. Xiao, Y. Cheng, L. Zhao, C. He, Z. Tang and X. Chen, *J. Mater. Chem.*, 2011, **21**, 11383–11391.
- L. Yin, H. Tang, K. H. Kim, N. Zheng, Z. Song, N. P. Gabrielson, H. Lu and J. Cheng, *Angew. Chem., Int. Ed.*, 2013, **52**, 9182–9186.
- S. Huang, Y. Chen, S. Ma and H. Yu, *Angew. Chem., Int. Ed.*, 2018, **57**, 12524–12528.
- H. I. Lee, W. Wu, J. K. Oh, L. Mueller, G. Sherwood, L. Peteanu, T. Kowalewski and K. Matyjaszewski, *Angew. Chem., Int. Ed.*, 2007, **46**, 2453–2457.
- S. Ji, L. Xu, X. Fu, J. Sun and Z. Li, *Macromolecules*, 2019, **52**, 4686–4693.
- X. He, J. Fan, J. Zou and K. L. Wooley, *Chem. Commun.*, 2016, **52**, 8455–8458.
- D. Huesmann, K. Klinker and M. Barz, *Polym. Chem.*, 2017, **8**, 957–971.
- T. J. Deming, *Chem. Rev.*, 2016, **116**, 786–808.
- H. Tang and D. Zhang, *Biomacromolecules*, 2010, **11**, 1585–1592.
- Y. Zhang, H. Lu, Y. Lin and J. Cheng, *Macromolecules*, 2011, **44**, 6641–6644.
- J. Sun and H. Schlaad, *Macromolecules*, 2010, **43**, 4445–4448.
- K. S. Krannig and H. Schlaad, *J. Am. Chem. Soc.*, 2012, **134**, 18542–18545.
- J. Yuan, Y. Zhang, Y. Sun, Z. Cai, L. Yang and H. Lu, *Biomacromolecules*, 2018, **19**, 2089–2097.
- J. Zhou, P. Chen, C. Deng, F. Meng, R. Cheng and Z. Zhong, *Macromolecules*, 2013, **46**, 6723–6730.
- J. R. Kramer and T. J. Deming, *Biomacromolecules*, 2012, **13**, 1719–1723.
- C. Ge, L. Zhao, Y. Ling and H. Tang, *Polym. Chem.*, 2017, **8**, 1895–1905.
- H. Lu, Y. Bai, J. Wang, N. P. Gabrielson, F. Wang, Y. Lin and J. Cheng, *Macromolecules*, 2011, **44**, 6237–6240.
- G. S. Hartley, *Nature*, 1937, **140**, 281–281.
- H. M. Bandara and S. C. Burdette, *Chem. Soc. Rev.*, 2012, **41**, 1809–1825.
- W. Xiong, H. Zhou, C. Zhang and H. Lu, *Chin. Chem. Lett.*, 2017, **28**, 2125–2128.
- L. Sun, F. Gao, D. Shen, Z. Liu, Y. Yao and S. Lin, *Polym. Chem.*, 2018, **9**, 2977–2983.
- J. A. Lv, Y. Liu, J. Wei, E. Chen, L. Qin and Y. Yu, *Nature*, 2016, **537**, 179–184.
- M. Yamada, M. Kondo, J. Mamiya, Y. Yu, M. Kinoshita, C. J. Barrett and T. Ikeda, *Angew. Chem., Int. Ed.*, 2008, **47**, 4986–4988.
- B. Soberats, E. Uchida, M. Yoshio, J. Kagimoto, H. Ohno and T. Kato, *J. Am. Chem. Soc.*, 2014, **136**, 9552–9555.
- W.-C. Xu, S. Sun and S. Wu, *Angew. Chem., Int. Ed.*, 2019, **58**, 9712–9740.
- Y. Yue, Y. Norikane, R. Azumi and E. Koyama, *Nat. Commun.*, 2018, **9**, 3234.
- H. Nie, S. Li, S. Qian, Z. Han and W. Zhang, *Angew. Chem., Int. Ed.*, 2019, **58**, 11449–11453.
- P. Li, G. Xie, X. Y. Kong, Z. Zhang, K. Xiao, L. Wen and L. Jiang, *Angew. Chem., Int. Ed.*, 2016, **55**, 15637–15641.
- J. Wu, B. Xu, Z. Liu, Y. Yao, Q. Zhuang and S. Lin, *Polym. Chem.*, 2019, **10**, 4025–4030.
- W. Wang, D. Shen, X. Li, Y. Yao, J. Lin, A. Wang, J. Yu, Z. L. Wang, S. W. Hong, Z. Lin and S. Lin, *Angew. Chem., Int. Ed.*, 2018, **57**, 2139–2143.
- W. A. R. Vanheeswijk, M. J. D. Eenink and J. Feijen, *Synthesis*, 1982, 744–747.
- C.-a. Yang, H. Xie, S. Chen and H. Zhang, *Liq. Cryst.*, 2013, **40**, 1487–1502.
- H.-L. Xie, S.-J. Wang, G.-Q. Zhong, Y.-X. Liu, H.-L. Zhang and E.-Q. Chen, *Macromolecules*, 2011, **44**, 7600–7609.

- 50 H. Lu, J. Wang, Y. Bai, J. W. Lang, S. Liu, Y. Lin and J. Cheng, *Nat. Commun.*, 2011, **2**, 206.
- 51 A. J. Rhodes and T. J. Deming, *ACS Macro Lett.*, 2013, **2**, 351–354.
- 52 A. Y. Shaikh, S. Das, D. Pati, V. Dhaware, S. Sen Gupta and S. Hotha, *Biomacromolecules*, 2014, **15**, 3679–3686.
- 53 H. Li, S. J. Shen, C. L. Zhu and H. Xu, *J. Am. Chem. Soc.*, 2019, **141**, 9415–9421.